Structure and Luminescence of 2D Dilute Magnetic Semiconductors: $Cd_{1-x}Mn_xSe{\cdot}L_{0.5}$ (L = Diamines)

Jun Lu, Shuo Wei, Weichao Yu, Houbo Zhang, and Yitai Qian*

Structure Research Laboratory and Department of Chemistry, University of Science and Technology of China, Hefei, Anhui, 230026, People's Republic of China

Received September 22, 2004. Revised Manuscript Received January 22, 2005

The two-dimensional (2D) dilute magnetic semiconductors $Cd_{1-x}Mn_xSe{\cdot}L_{0.5}$ (L = ethylenediamine, or *en*, and 1,6-hexanediamine, or *hda*, $x = 0-0.8$) were synthesized in an autoclave at 120 °C. Ab initio structure solution from X-ray powder diffraction reveals the host compound $CdSe{\cdot}hda_{0.5}$ (space group, *Pbca*, $a = 6.8852$ Å, $b = 6.7894$ Å, $c = 27.4113$ Å) is structurally analogous to $CdSe{\cdot}en_{0.5}$, except for a subtle difference in alignment of aliphatic diamine ligands—the *hda* molecule deflects from the *c* axis and inclines toward the *b* axis. $CdSe{\cdot}L_{0.5}$ shows well-defined UV absorption and emission peaks, which is attributed to a 2D exciton band edge transition due to size confinement effect in the *c* direction and the only photoemission level is the 2D exciton ground state with a long lifetime (7 μs) and intrinsic line width (177 meV) at room temperature. When Cd^{2+} is partly substituted by Mn^{2+}, a strong Mn^{2+}-related luminescence peak at 2.12 eV (584 nm) is obtained at room temperature, which can be assigned to Mn^{2+} internal transition ($^4T_1 \rightarrow {}^6A_1$); its excitation peak overlaps with the photoemission peak of the 2D exciton ground state which indicates that the Mn^{2+} emission is driven by the 2D exciton ground-state transition. For $x = 0.02$, the photoluminescence intensity of $Cd_{1-x}Mn_xSe{\cdot}hda_{0.5}$ reaches maximum and enhances 28 times compared with that of $Cd_{1-x}Mn_xSe{\cdot}en$. When $x < 0.05$, the Mn^{2+} luminescence is a characteristic single-exponential decay process with a well-defined constant lifetime of 375 μs. Electron spin resonance spectra show that Mn^{2+} substitutes Cd^{2+} ion and forms a $[MnSe_3N]$ coordination tetrahedron and that there are isolated Mn^{2+} luminescence centers in $Cd_{1-x}Mn_xSe{\cdot}hda_{0.5}$ ($x < 0.05$), which is the key factor for their stronger luminescence character compared to $Cd_{1-x}Mn_xSe{\cdot}en_{0.5}$.

1. Introduction

Manganese-doped II−VI group compounds are typical diluted magnetic semiconductors (DMS), which have magnetic properties resulting from the paramagnetic Mn ion and the optical and electrical properties mostly derived from the host semiconductor lattice. Because of the s,p−d exchange interaction between band electron/hole and Mn^{2+} $3d^5$ electron,[1−4] the DMS show outstanding magneto-optical properties such as giant Faraday rotation effect near the band edge, giant exciton Zeeman splitting, and a magnetic polaron state.[5−7] These properties make it possible to fabricate high-performance microstructures of optoelectronic devices. Recently, there were considerable interests in the research on the nanostructures of DMS (quantum wells, quantum wires, and quantum dots), which were expected to show varieties of the optical phenomena due to the coexistence of quantum confinement effect and the exchange interaction.[8] For instance, ZnS:Mn showed a Mn^{2+} internal transition ($^4T_1 \rightarrow {}^6A_1$) luminescence at 584 nm with a high quantum efficiency. It was found that the optical properties of Mn^{2+}-doped CdSe nanocrystals are similar to those of undoped nanocrystals in an external magnetic field,[9] and 2D $Cd_{1-x}Mn_xSe$ quantum wells exhibit giant magnetooptical effects and ultrafast exciton dynamics.[10,11]

The diamine-intercalated layered compounds, including $ZnE{\cdot}L_{0.5}$, $CdE{\cdot}L_{0.5}$, $MnSe{\cdot}L_{0.5}$, and $Zn_{1-x}Mn_xSe{\cdot}L_{0.5}$ (E = Se or Te and L = aliphatic diamines), are a novel type of inorganic/organic (I/O) hybrid structures.[12−16] It has been found that $Zn_{1-x}Mn_xSe{\cdot}L_{0.5}$ has a strong Mn^{2+}-related luminescence and luminescent-enhancement effect for longer

* To whom correspondence may be addressed. E-mail: ytqian@ustc.edu.cn.

(1) Bartholomew, D. U.; Furdyna, J. K.; Ramdas, A. K. *Phys. Rev. B* **1986**, *34*, 6943.
(2) Oh, E.; Bartholomew, D. U.; Ramdas, A. K.; Furdyna, J. K.; Debska, U. *Phys. Rev. B* **1988**, *38*, 13183.
(3) Dai, N.; Luo, H.; Zhang, F. C.; Samarth, N.; Dobrowolska, M.; Furdyna, J. K. *Phys. Rev. Lett.* **1994**, *67*, 3824.
(4) Jonker, B. T.; Liu, X.; Chou, W. C.; Petrou, A.; Warnock, J.; Krebs, J. J.; Prinz, G. A. *J. Appl. Phys.* **1991**, *69*, 6098.
(5) Furdyna, J. K. *J. Appl. Phys.* **1988**, *64*, R29.
(6) Alonso, R. G.; Suh, E.-K.; Ramdas, A. K.; Samarth, N.; Luo, H.; Furdyna, J. K. *Phys. Rev. B* **1989**, *40*, 3720.
(7) Goede, O.; Heimbrodt, W. *Phys. Stat. Sol.* **1988**, *146*, 11.
(8) Takahashi, N.; Takabayashi, K.; Shirado, E.; Souma, I.; Shen, J. X.; Oka, Y. *J. Cryst. Growth* **2000**, *214/215*, 183.
(9) Mikulec, F. V.; Kuno, M.; Bennati, M.; Hall, D. A.; Griffin, R. G.; Bawendi, M. G. *J. Am. Chem. Soc.* **2000**,*122*, 2532.
(10) Oka, Y.; Yanata, K.; Okamoto, H.; Takahashi, M.; Shen, J. *Solid-State Electron.* **1998**, *42*, 1267.
(11) Oka, Y. *Phys. Solid State* **1998**, *40*, 778.
(12) Huang, X.; Li, J. *J. Am. Chem. Soc.* **2000**, *122*, 8789.
(13) Huang, X.; Li, J. *Chem. Mater.* **2001**, *13*, 3754.
(14) Heuling, H. R., IV; Huang, X.; Li J.; Yeun, T.; Lin, C. L. *Nano Lett.* **2001**, *1*, 521.
(15) Huang, X.; Li, J.; Zhang, Y.; Mascarenhas, A. *J. Am. Chem. Soc.* **2003**, *125*, 7049. Therein the reported lattice constants of powder $CdSe{\cdot}en_{0.5}$ were $a = 7.0949$, $b = 6.795$, $c = 16.7212$ Å, and $V = 806.17$ Å^3, and those of powder CdSe·0.5pda were $a = 20.6660$, $b = 6.8900$, and $c = 6.7513$ Å.
(16) Deng, Z. X.; Li, L.; Li, Y. *Inorg. Chem.* **2003**, *42*, 2331. Therein, the reported lattice constants of single-crystal $CdSe{\cdot}en_{0.5}$ were $a = 7.0848$, $b = 6.7856$, $c = 16.6940$ Å, and $V = 802.56$ Å^3.

10.1021/cm048339y CCC: $30.25 © 2005 American Chemical Society
Published on Web 03/11/2005

diamines molecules.[17] Optical diffuse reflectance measurements indicated that CdSe·$en_{0.5}$ (*en* = ethylenediamine) has a band gap of 3.41 eV (364 nm) with a large blue shift (~1.67 eV) compared with that of bulk CdSe (1.74 eV), which can be attributed to the quantum confinement effect of the [CdSe] monolayers. This blushift makes the band gap value of CdSe·$en_{0.5}$ greater than the energy of Mn^{2+} internal transition ($^4T_1 \rightarrow {}^6A_1$, typical of 2.12 eV) and provides possibility for obtaining the Mn^{2+}-related Stokes luminescence in Mn-doped CdSe·$L_{0.5}$. Except for the fact that the denity functional approximation (DFA) calculation reveals that the optical characters of these hybrid compounds are determined by the inorganic layer, so far, no other theoretical research has been reported on their band gap structure and optical properties.

For MSe·$L_{0.5}$ (M = Zn, Mn), crystallographic analysis revealed that these compounds consist of [MSe] 2D monolayer interconnected by diamine molecules.[13] In the lattice of ZnSe·$en_{0.5}$, the [ZnSe] monolayer could be viewed as a 2D superlattice of $\sqrt{3}a \times c$ of the (110) plane of wurtzite-type ZnSe,[17] and CdSe·$en_{0.5}$ is isostrucural with Zn and Mn counterparts.[16] Although the strong quantum confinement effect was expected, no study has been reported on the exciton transition of [MSe] monolayer, Mn^{2+} emission, and luminescence decay in $Cd_{1-x}Mn_xSe·L_{0.5}$.

In this study, 2D DMS $Cd_{1-x}Mn_xSe·L_{0.5}$ (L = *en* and 1,6-hexadiamine (*hda*), $x = 0-0.8$) were synthesized in an autoclave at 120 °C. Ab initio structure solution from powder diffraction showed that the CdSe·$hda_{0.5}$ with a long *c* period ($c = 27.4$ Å) is structurally analogous to CdSe·$en_{0.5}$ ($c = 16.7$ Å) except that all *hda* ligands deflect from the *c* axis and incline to the *b* axis. UV absorption/emission features were observed at room temperature for CdSe·$hda_{0.5}$, which were assigned to the 2D exciton ground-state transition. $Cd_{1-x}Mn_xSe·hda_{0.5}$ gave Mn^{2+} emission at 2.12 eV (584 nm) at room temperature, which was excited by the 2D exciton ground-state transition. Luminescence decay curves showed Mn^{2+} emission is a typical single-exponential decay process with a constant lifetime of 375 μs ($x < 0.05$). The Mn^{2+} luminescence intensity of $Cd_{1-x}Mn_xSe·L_{0.5}$ ($x = 0.02$) exhibited enhancement effect for L = *hda*. The electron spin resonance spectra were employed to obtain an insight about the site symmetry of Mn^{2+} ions and the luminescence-enhancement effect.

2. Experimental Section

2.1. Synthesis. All chemicals are of analytical-grade purity, purchased from Shanghai Chemical Reagent Co., Ltd, and without further purification. CdSe·$L_{0.5}$ (L = *en* and *hda*) were solvothermally synthesized as follows. $Cd(CH_3CO_2)_2·2H_2O$ (5 mmol) and 5 mmol of selenium powder were dissolved into 50 mL of solvent L. The mixture was sealed into 60 mL of Teflon-lined stainless steel autoclave and heated at 120 °C for 7 days, then cooled naturally. The products were washed with distilled water and absolute ethanol and then dried in a vacuum at 60 °C for 2 h. $Mn(CH_3CO_2)_2·4H_2O$ was used as the Mn-doping source, and $Cd_{1-x}Mn_xSe·L_{0.5}$ (x = 50 ppm −0.8) was prepared in a similar procedure with various molar ratio of Cd^{2+}:Mn^{2+}.

2.2. Component Analysis. Elemental analysis of C, H, and N weight percentages of CdSe·$L_{0.5}$ (using a Perkin-Elmer 2400 elemental analyzer) were 5.688, 1.819, 6.223 (calcd. 5.429, 1.821, 6.326 wt %) for L = *en* and 14.74, 3.233, 5.525 (calcd.14.443, 3.232, 5.614 wt %) for L = *hda*. It can be seen that the obtained data of C, H, and N are consistent with the calculated values in the range of experimental error (±0.3%). Therefore, the chemical stoichiometry of CdSe·$L_{0.5}$ can be regarded as accurate. Inductively coupled plasma atomic emission spectra (ICP-AES, using an Atomscan Advantage Spectrometer, Therma Jarrell Ash Co.) were used to determine the Mn contents of $Cd_{1-x}Mn_xSe·L_{0.5}$. For L = *hda*, Cd^{2+}:Mn^{2+} (molar ratio) = 49/1, 19/1, 9/1, and 1/4, the determined Mn contents were $x = 0.0149$ (49/1), 0.0488 (19/1), 0.0829 (9/1), and 0.791 (1/4), respectively. For L = *en*, Cd^{2+}:Mn^{2+} = 19/1, the determined Mn content was $x = 0.045$. Therefore, the Mn^{2+}-doping solvothermal reactions for $Cd_{1-x}Mn_xSe·L_{0.5}$ can be regarded as quantitative.

2.3. Structure Analysis. The powder X-ray diffraction (XRD) pattern of CdSe·$hda_{0.5}$ for ab initio structure solution was collected on a MXP 18 AHF X-ray diffractometer (MAC Science Co. Ltd., Japan) with a diffracted beam graphite monochromator and operating at 40 kV and 100 mA (Cu Kα, $\lambda = 1.54184$ Å). Data collection was carried out in a step-scan mode with a step-size of 0.02° in the angular range of 4.00−100.00°. The pattern was indexed by the TREOR[18a] method using program Fullprof[18b] to the orthorhombic system with unit cell dimensions of $a = 6.8852$, $b = 6.7894$, $c = 27.4113$ Å, $V = 1281.379$ Å^3. The space group was assumed to be *Pbca*, and $Z = 8$. The crystal structure was solved by direct methods with program EXPO.[19] Refinement of the 4800 observations (666 reflections) of the pattern was carried out by the Rietveld method, based on a stoichiometry of CdSe·$hda_{0.5}$. The resulting unit cell parameters as well as the atomic parameters and space groups were input as initial values for Rietveld full-pattern refinement in program GSAS.[20] After the initial refinement of the scale, background (function #2, Cosine Fourier series 8 terms), and unit cell parameters, profile function #2 was selected (pseudovoigt function with profile coefficients of 18 terms for Simpson's rule integration[21]) and the profile parameters LX, LY, trns, asym, shft, GP, stec, ptec, sfec, were refined one by one. The preferred orientation corrections were made by applying spherical harmonics function, and atomic positions were refined finally. Hydrogen atoms and absorption effects were not included in the refinement. The details of the Rietveld refinement are described in Table 1. Non-hydrogen atomic positional parameters are given in Table 2. The reliability indices, a measure of how well the calculated pattern and structure agree with the observed data, are as follows: $R_p = 0.0675$, $R_{wp} = 0.1567$, and $R_F = 0.1045$.[22]

2.4. Optical Absorption and Photoluminescence (PL) Spectra. The optical absorption spectra of the CdSe·$L_{0.5}$ powders dispersed in ethanol were recorded on a Shimadzu 2401pc UV/vis spectrometer. The PL emission and excitation spectra of CdSe·$L_{0.5}$ and $Cd_{1-x}Mn_xSe·L_{0.5}$ powders were obtained at room temperature using a Perkin-Elmer LS 55 luminescence spectrometer (Perkin-Elmer

(17) Lu, J.; Wei, S.; Peng, Y. Y.; Yu, W.; Qian, Y. T. *J. Phys. Chem. B* **2003**, *107*, 3027.

(18) (*a*) Werner, P. E.; Eriksson, L.; Westdahl, M. *J. Appl. Crystallogr.* **1985**, *18*, 367. (*b*) Roisnel, T.; Rodriguez-Carvajal, J. *WinPLOTR*; May, 2003.

(19) Altomare, A.; Carrozzini, B.; Cascarano, G.; Giacovazzo, C.; Guagliardi, A.; Moliterini, A. G. G.; Rizzi, R.; Bura, M. C.; Polidore G.; Camalli, M. *EXPO*. A package for full-pattern decomposition and for solving crystal structure by direct methods.

(20) VonDreele, R. B.; Larson, A. C. *GSAS, General Structure Analysis System*; Los Alamos National Laboratory: Los Alamos, NM, 2001.

(21) (a) Howard, C. J. *J. Appl. Crystallgr.* **1982**, *15*, 615. (b) Thompson, P.; Cox, D. E.; Hastings, J. B. *J. Appl. Crystallgr.* **1987**, *20*, 79.

(22) Details of powder pattern indexing result and Rietveld refinement plot see Supporting Information.

Table 1. Crystallographic Data for CdSe·*hda*$_{0.5}$

empirical formula	C_3H_8NCdSe
Fw	1995.79
space group	*Pbca* (No. 61)
a, *b*, *c* (Å)	6.8852, 6.7894, 27.4113
V (Å^3)	1281.379
Z	8
T (K)	293(2)
λ (Å)	1.54056, 1.54439
ρ_{calc}(g cm^{-3})	2.586
pattern range (2θ deg)	4−100
step size (2θ deg)	0.02
step scan time (s)	2
no. contributing reflns (Kα_1 + Kα_2)	666
no. refinement parameters	66
R_{wp}	0.1567
R_p	0.0675
$R(F^2)$	0.1045

Table 2. Atomic Coordinates for CdSe·*hda*$_{0.5}$

atom	*x*	*y*	*z*
Cd	0.1000(1)	0.1925(6)	0.7178(5)
Se	−0.0473(6)	0.3154(1)	0.7994(9)
N	−0.0650(2)	0.3613(1)	0.6552(2)
C(1)	0.0369(6)	0.5265(6)	0.4308(4)
C(2)	0.5359(5)	0.4240(3)	0.9817(8)
C(3)	−0.0021(4)	0.6939(9)	0.3949(2)

Instruments Co., Ltd., USA) with Rhodamine 101 as the interior standard for luminescence intensity, and measurement conditions were identical in all cases; therefore relative intensities can be compared. Luminescence decay curves were obtained by a delay method using a Jobin Yvon Fluorolog 3-TAU luminescence spectrometer (Jobin Yvon Instruments Co., Ltd., France) at room temperature and excitation pulse was produced from a 450-W Xe flash lamp.

2.5. Electron Spin Resonance (ESR) Spectra of $Cd_{1-x}Mn_xSe$·$L_{0.5}$. Room-temperature ESR spectra of $Cd_{1-x}Mn_xSe$·$L_{0.5}$ powder were obtained using a JEOL JES-FA200 ESR spectrometer (300 K, 9.063 GHz, X-band). Microwave power employed was 5 mW; sweep width ranged from 2000 to 4000 G. Modulation frequency and modulation amplitude were 100 kHz and 3.5 G, respectively.

3. Results and Discussion

3.1. Structure Description. Figure 1 illustrates a structure view of CdSe·*hda*$_{0.5}$ along the *a* axis, which is a 3D network with [CdSe] monolayer interconnected by bridging *hda* molecules with all-trans configuration. The [CdSe] monolayer with a thickness of 0.27 nm and the [$CdSe_3N$] coordination tetrahedra are structurally analogous to CdSe·*en*$_{0.5}$.[16] And the [CdSe] monolayer can also be regarded as a shrunken 2D superlattice ($\sqrt{3}a \times c$) of the (110) plane of wurtzite-type CdSe.[17,22] On the other hand, besides the increase of interlayer distance between the [CdSe] monolayer as expected, a subtle structural difference is that all the *hda* molecules align with deflection from the *c* axis and inclination toward the *b* axis, while the *en* molecules are parallel with the *c* axis and align vertically to bridge Cd atoms in CdSe·*en*$_{0.5}$. The [CdSe] monolayers supply a 2D system of valence band electrons/holes, which will result in strong quantum-confined effect and exciton transition as described below.

3.2. Absorption and Luminescence Spectroscopy of Undoped CdSe·*hda*$_{0.5}$. Figure 2a shows the room-temperature absorption (1) and emission (2) spectra of the undoped

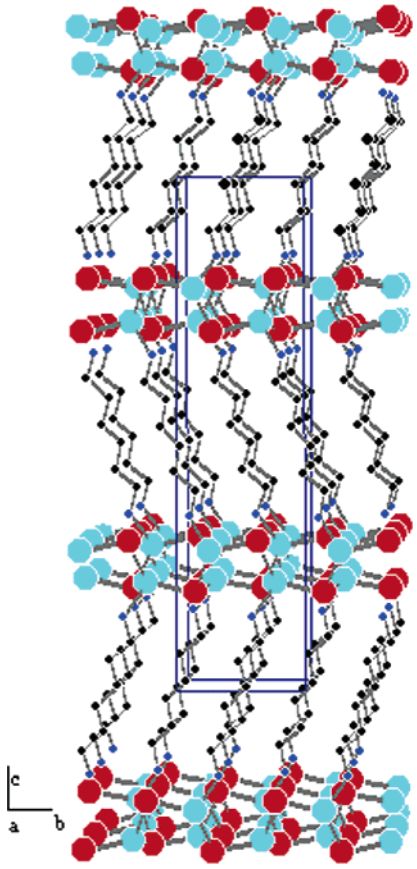

Figure 1. Structure view of CdSe·*hda*$_{0.5}$ shown along the *a* axis with the unit cell outlined. The large cyan and red spheres are Cd and Se atoms; small black and blue spheres are C and N atoms, respectively.

CdSe·*hda*$_{0.5}$ which has a well-defined absorption peak at 354 nm (3.50 eV) and a sharp emission peak at 362 nm (3.43 eV) with a Stokes shift of 70 meV and a full width at half-maximum of 177 meV. Higher energy absorption features can also be resolved at 313 nm (3.96 eV) and 342 nm (3.62 eV) in the absorption spectrum. CdSe·*en*$_{0.5}$ shows similar absorption/emission spectra,[22] which indicate that the UV absorption/emission originate from the valence electron transition process in the [CdSe] monolayer, while independent of the length of diamine molecules. The [CdSe] monolayer, separated by aliphatic diamine molecules, has a dimension of 0.27 nm in the *c* direction, far less than the exciton Bohr radius of CdSe (5.6 nm), which results in the confinement of electron/hole motion in the *c* direction and the formation of 2D exciton analogous to semiconductor superlattice.[23] It is known that, due to 3D quantum confinement, high-quality CdSe colloidal nanocrystals exhibit band-edge exciton absorption/emission with several tens of millielectonvolts of Stokes shift, which is also similar to the current result. Therefore, the UV absorption/emission peaks can be assigned to a *c*-confined 2D exciton transition of the [CdSe] monolayer, and its transition energy of 2D exciton is greater than that of the smallest CdSe colloidal nanocrystals available (2.6 nm, 2.5 eV[9]) due to the strong size confinement (0.27 vs 5.6 nm). Compared with the diffuse reflectance spectra of CdSe·*en*$_{0.5}$,[15] the absorption spectrum 1 shows the same peak at ∼3.4−3.5 eV but a very long tail

(23) Yoffe, A. D. *Adv. Phys.* **1993**, *42*, 173.

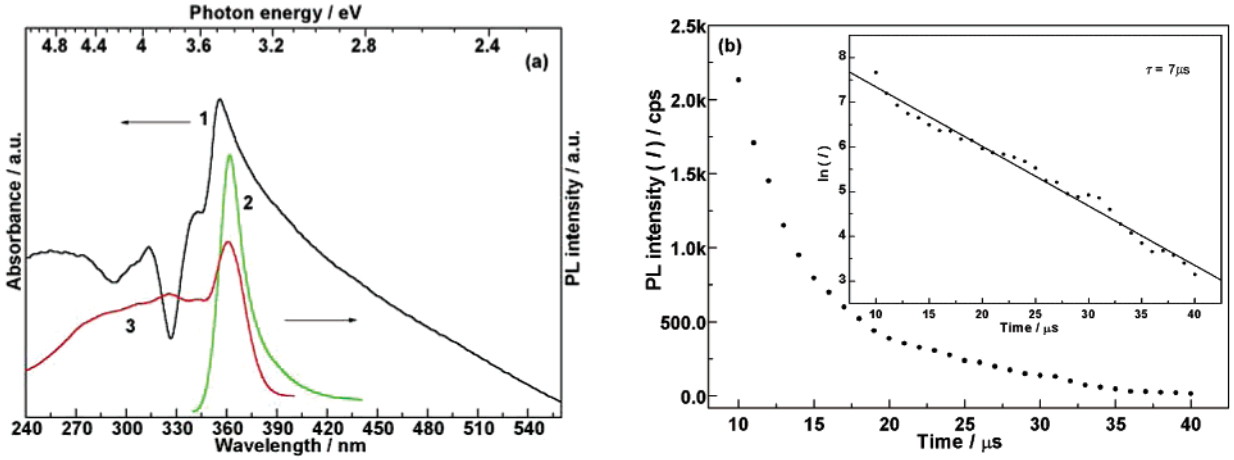

Figure 2. (a) *c*-Confined 2D exciton absorption (1) and emission (2) spectra of CdSe·$hda_{0.5}$ (excitation wavelength 313 nm). For comparison, the excitation spectrum (3) of Mn^{2+} emission (584 nm) in $Cd_{0.98}Mn_{0.02}Se$·$hda_{0.5}$ is also shown. (b) Decay curve of 2D exciton luminescence; the inset in (b) is the ln $I-t$ plot to obtain the luminescence lifetime.

to the red, which does not occur in the former. An unavoidable cause for this difference is the specimen measurement state (polycrystalline powder is used in diffuse reflectance experiments, here is the microcrystals suspension). Therefore, it can be expected that the long red tail is related to the interaction between the lamellar polycrystalline particles and dispersive solvent (ethanol), in which the affection of surface states and defects cannot be absolutely excluded for they have been theoretically predicted in ZnTe·$en_{0.5}$ by density functional theory within local density approximation.[12]

On the other hand, the 3.43-eV (362-nm) emission peak excited by the 3.96-eV (313-nm) photons can also be stimulated by any photons with energy higher than 3.43 eV. This implies that a 2D exciton ground state is the only photoemission exciton energy level in the UV spectral regime. Furthermore, the *c* dimension of [CdSe] monolayer is identified in the whole lattice and a size-selective treatment is not needed, which is indispensable for colloidal nanocrystals to minimize inhomogeneous spectral broadening and obtain well-defined exciton absorption/emission peaks. Therefore, the peak width of 177 meV for 3.43 eV of emission totally originates from intrinsic homogeneous broadening and implies a narrow 2D exciton ground state in the band gap.

The photoemission process of 2D exciton ground state was probed by luminescence decay dynamics, and the decay curve is shown in Figure 2b, which can be fitted into a single-exponential decay with a lifetime of 7 μs (inset)[22] within the detectable decay time scale (>1 μs). This is comparable with the band-edge dark exciton lifetime (~ 1 μs at 10 K) of wurtzite CdSe nanocrystals and far exceeds that of their bulk counterpart (~ 1 ns at 4 K).[24] In CdSe nanocrystals, it has been established that the long radiative lifetime of band-edge dark exciton states (dipole forbidden excitons with total angular momentum projection $F_m = \pm 2$) results from the intrinsic crystal/shape anisotropy (nonspherical morphology and wurtzite structure lift the degeneracy of band edge excitons) and confinement-enhanced electron−hole exchange interaction.[25] The enhanced exchange effect due to carrier confinement was also confirmed in GaAs/GaAlAs quantum wells,[26] and exchange interaction splits the localized exciton in porous silicon, which results in slow radiative states at lower energy.[27] The [CdSe] monolayer in CdSe·$L_{0.5}$ has strong quantum confinement in the *c* direction and is structurally derived from wurtzite CdSe ($a \approx \sqrt{3}a_W$, $b \approx c_W$, a_W, and c_W are lattice parameters of wurtzite CdSe). Furthermore, the 2D excition ground state has a comparable radiative lifetime with 3D-confined CdSe QDs; therefore, it is possible that the 2D exciton states were modified by similar factors. Of course, it is absolutely necessary that an in-depth study on the 2D exciton PL at low temperature, and/or in magnetic field, and luminescence dynamics on a sub-microsecond scale be performed, which would be favorable to elucidate the origin of the unique long lifetime 2D excition. On the other hand, for these undoped compounds, no intrinsic luminescence peak at 584 nm was found with excitation at 362 nm.

3.3. Mn^{2+} Luminescence Spectroscopy of $Cd_{1-x}Mn_x$-Se·$hda_{0.5}$. Figure 3 shows the PL excitation (left) and emission (right) spectra of the isomorphous $Cd_{1-x}Mn_xSe$·$L_{0.5}$ ($x = 0.02$), where the spectra for L = *en* was magnified by 5 times for comparison. Both of them show emission peaks at 2.12 eV (584 nm) with a half width of 200 meV, which can be assigned to the typical Mn^{2+} internal transition ($^4T_1 \rightarrow {}^6A_1$).[28,29] The half widths of the emission peaks (200 meV) indicate that the inhomogeneous broadening is unobvious, that is, Mn^{2+} ions have homogeneous coordination environments. In the excitation spectrum (Figure 2a, curve

(24) (*a*) Crooker, S. A.; Barrick, T.; Hollingsworth, J. A.; Klimov, V. I. *Appl. Phys. Lett.* **2003**, *82*, 2793. (*b*) Takabayashi, K.; Takahashi, N.; Yagi, I.; Souma, I.; Shen, J. X.; Oka, Y. *J. Lumin.* **2000**, *87*−*89*, 347.
(25) (*a*) Nirmal, M.; Norris, D. J.; Kuno, M.; Bawendi, M. G.; Efros, Al. L.; Rosen, M. *Phys. Rev. Lett.* **1995**, *75*, 3728. (*b*) Efros, Al. L.; Rosen, M.; Kuno, M.; Nirmal, M.; Norris, D. J.; Bawendi, M. G. *Phys. Rev. B* **1996**, *54*, 4843. (*c*) Norris, D. J.; Efros, Al. L.; Rosen, M.; Bawendi, M. G. *Phys. Rev. B* **1996**, *53*, 16347.
(26) (*a*) Stark, J. B.; Knox, W. H.; Chemla, D. S. *Phys. Rev. B* **1992**, *46*, 7919. (*b*) Potemski, M.; Maan, J. C.; Fasolino, A.; Ploog, K.; Weimann, G. *Surf. Sci.* **1990**, *229*, 151.
(27) Calcott, P. D. J.; Nash, K. J.; Canham, L. T.; Kane, M. J.; Brumhead, D. *J. Lumin.* **1993**, *57*, 257.
(28) Norris, D. J.; Yao, Nan; Charnock, F. T.; Kennedy, T. A. *Nano Lett.* **2001**, *1*, 3.
(29) Norman, T. J.; Magana, D., Jr.; Wilson, T.; Burns, C.; Zhang, J. Z.; Cao, D.; Bridges, F. *J. Phys. Chem. B* **2003**, *107*, 6309.

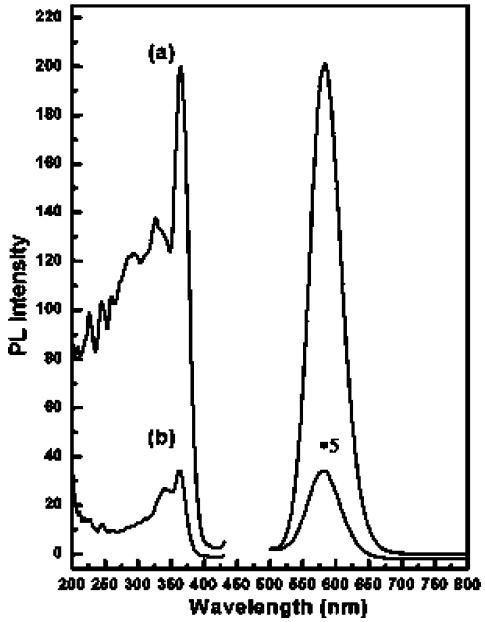

Figure 3. The PL excitation and emission spectra of $Cd_{1-x}Mn_xSe{\cdot}L_{0.5}$ ($x = 0.02$): (a) L = *hda* and (b) L = *en*, where the spectra have been magnified by 5 times.

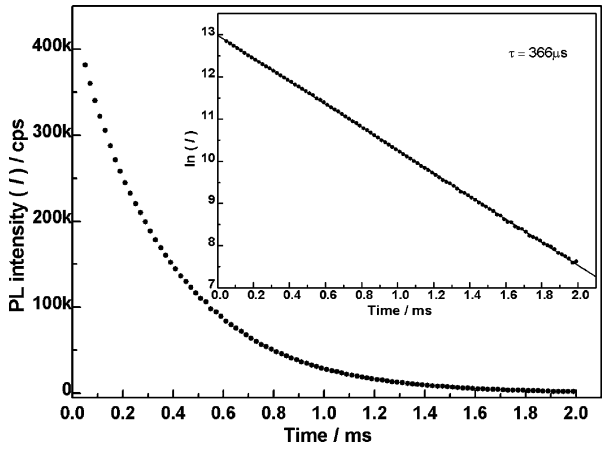

Figure 4. Mn^{2+} luminescence decay curve of $Cd_{0.98}Mn_{0.02}Se{\cdot}hda_{0.5}$. The inset is the ln*I*−*t* plot. The solid circle and line are the experimental and fitted curves, respectively.

3), the narrow excitation peak at 3.41 eV (364 nm) is consistent with the 2D exciton emission peak in $CdSe{\cdot}hda_{0.5}$ (curve 2), indicating that the Mn^{2+} emission is driven by the 2D exciton ground-state transition of [CdSe] monolayer. The Mn^{2+} emission intensity is 2 orders of magnitude greater than that of 2D exciton at 362 nm, which shows that Mn^{2+} is a high-effective acceptor for 2D exciton ground-state transition energy.[30] Compared with that of L = *en* (7.2), the emission intensity increases 28 times for L = *hda* (201), which shows the luminescence-enhancement effect and implies that the long period in *c* direction is more favor for the enhancement of Mn^{2+}-related emission, which was previously found in $Zn_{1-x}Mn_xSe{\cdot}L_{0.5}$.[17]

The Mn^{2+} luminescence decay curve of $Cd_{0.98}Mn_{0.02}Se{\cdot}hda_{0.5}$ is shown in Figure 4; the plot of ln *I* vs decay time (*t*) could be well-fit into a typical single-exponential decay process with a lifetime of 366 μs (Figure 4, inset). This value

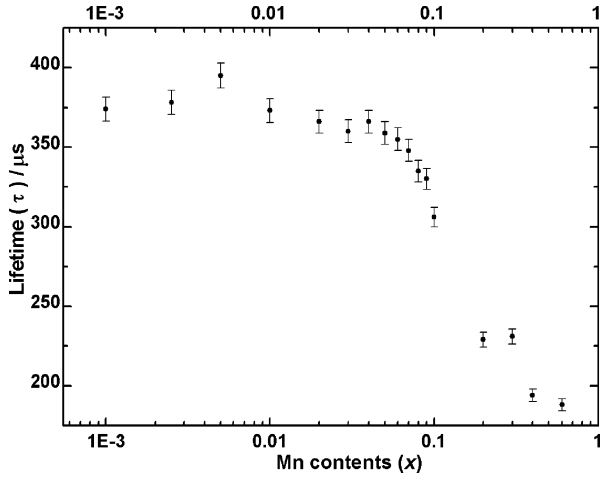

Figure 5. Mn^{2+} luminescence lifetime vs Mn contents (*x*) dependence of $Cd_{1-x}Mn_xSe{\cdot}hda_{0.5}$.

is comparable with those of ZnSe:Mn, which are not well established and varied between 30 and 800 μs.[31] And the well-defined lifetimes show thermal quenching has no effect on the luminescence at room temperature. The Mn^{2+} contents dependence of lifetime (Figure 5) reveals, for *x* ranging from 0.001 to 0.05, the lifetime almost remains constant at 375 μs. Then it decreases slowly in the regime of 0.05−0.01 and drops to 300 μs at $x = 0.1$. for $x > 0.1$; the luminescence intensity decreases obviously, and the decay curve could not be fit into a single-exponential decay process within the time scale of 2 ms; the lifetime could only be estimated from the curve section less than 1 ms and reduces rapidly with the increasing Mn^{2+} contents and falls to 180 μs at $x = 0.6$, which indicates that concentration quench dominates luminescence and results in a complex decay process. It could be expected that the formation of exchange-coupled Mn^{2+} pairs for higher Mn^{2+} concentrations (>0.05 in the current study), and due to exchange interaction, the spin selection rule is partially lifted and the lifetime of the Mn^{2+} emission is reduced. This could explain the Mn^{2+} luminescence lifetimes of $Cd_{1-x}Mn_xSe{\cdot}hda_{0.5}$. But no redshift of Mn^{2+} emission is observed with increasing Mn^{2+} concentrations, which is an evidence for Mn^{2+} pair formation in CdSe:Mn. Therefore, it can be concluded that, when $x < 0.05$, the Mn^{2+} internal transition ($^4T_1 \rightarrow {}^6A_1$) emission is a typical isolated ion transition process without obvious exchange interaction.

3.4. ESR Spectroscopy of $Cd_{1-x}Mn_xSe{\cdot}hda_{0.5}$. It is known that the total electron spin of Mn^{2+} ($S = {}^5/_2$) is sensitive to changes of its coordination environment and modifies the crystal field via its spin Hamiltonian parameters; therefore the Mn^{2+} ESR spectra was used as a probe to study the Mn^{2+} coordination state and $Mn^{2+}-Mn^{2+}$ interaction in $Cd_{1-x}Mn_xSe{\cdot}L_{0.5}$.

In parts a and b of Figure 6, only a kind of signal, six well-resolved hyperfine lines, could be observed, which are from the ^{55}Mn nucleus ($I = {}^5/_2$) and correspond to the allowed transition ($\Delta m_S = \pm 1$, $\Delta m_I = 0$) where m_S and m_I are electron spin and nuclear spin quantum numbers, respectively. The hyperfine constant $A = 64.5 \times 10^{-4}$ cm^{-1} and

(30) Rigby, N. E.; Allen, W. E. *J. Lumin.* **1988**, *42*, 143.

(31) Suyver, J. F.; Wuister, S. F.; Kelly, J. J.; Meijerink, A. *Phys. Chem. Chem. Phys.* **2000**, *2*, 5445.

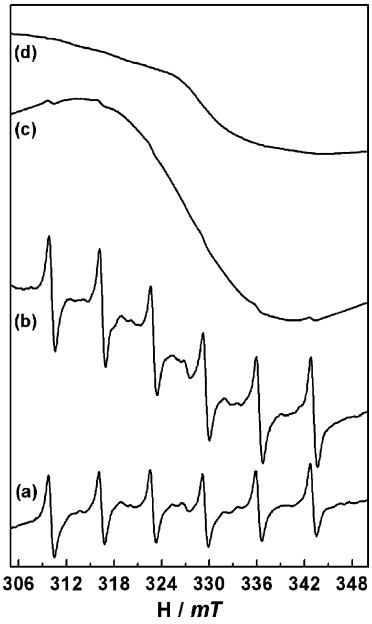

Figure 6. Room-temperature Mn^{2+} ESR spectra of $Cd_{1-x}Mn_xSe{\cdot}L_{0.5}$ powder specimens: (a) $x = 0.01$, L = *hda*; (b) $x = 0.02$, L = *hda*; (c) $x = 0.05$, L = *hda*; (d) $x = 0.02$, L = *en*.

line widths of 8 G are consistent with that of tetrahedral coordination Mn^{2+} in CdSe:Mn crystals,[32] which indicates that the doping Mn^{2+} ions substitute in a Cd^{2+} site, form $[MnSe_3N]$ coordination tetrahedra, and all the Mn^{2+} ions have a homogeneous coordination environment without $Mn^{2+}-Mn^{2+}$ interaction. Between the six intense lines, several weak lines (seven in Figure 6a) are observed which could be assigned to double spin transition ($\Delta m_S = \pm 1$, $\Delta m_I = \pm 1$) where both m_s and m_I change simultaneously.[32] For higher Mn concentration ($x = 0.05$, Figure 6c), the second type signal, a broad mainly symmetrical line (line width of 270 G), appears and originates from the electron spin−spin ($m_s = {}^1/_2 \rightarrow m_s = -{}^1/_2$) interactions, which indicates that $Mn^{2+}-Mn^{2+}$ interaction has been present,[33] and six weak hyperfine lines superimpose the broad main line, which implies that some isolated Mn^{2+} still exist in the monolayer. This is different from that in Figure 6d (L = *en*, for $x = 0.02$) where the six hyperfine lines completely disappear and a complex broad line (line width of 440 G) indicating that $Mn^{2+}-Mn^{2+}$ interaction dominates in $Cd_{0.98}Mn_{0.02}Se{\cdot}en_{0.5}$. An isolate Mn^{2+} is a strong luminescence center, and the enhancement of $Mn^{2+}-Mn^{2+}$ interaction due to their close proximity is responsible for the Mn^{2+} luminescence quench.[33] Acording to the ESR spectra, the luminescent-enhancement effect could be explained as isolated Mn^{2+} can more readily exist in $Cd_{1-x}Mn_xSe{\cdot}L_{0.5}$ lattice with a long *c* period (L = *hda*), that is, when the diamine molecules became longer, the interlayer distances of $[Cd_{1-x}Mn_xSe]$ layers increase and the interlayer $Mn^{2+}-Mn^{2+}$ interaction weakens, and the 2D-confined character of PL process become more prominent, which undoubtedly contribute to luminescent-enhancement effect. It seems that the intralayer $Mn^{2+}-Mn^{2+}$ interaction is also absent in $Cd_{1-x}Mn_xSe{\cdot}hda_{0.5}$ ($x < 0.02$) lattice, the reason to which is not very clear and need to study further.

4. Conclusion

In summary, 2D DMS $Cd_{1-x}Mn_xSe{\cdot}L_{0.5}$ (L = *en* and *hda*, $x = 0-0.8$) have been synthesized in an autoclave at 120 °C. According to the ab initio structure solution from powder XRD pattern, the host compound $CdSe{\cdot}hda_{0.5}$ (*Pbca*, $a = 6.8852$, $b = 6.7894$, $c = 27.4113$ Å) is structurally analogous to $CdSe{\cdot}en_{0.5}$ except that *hda* molecules deflect from the *c* axis and incline to the *b* axis to bridge two Cd atoms in the adjacent inorganic layer. The strong size confinement effect in the *c*-direction results in the formation of 2D exciton in $CdSe{\cdot}L_{0.5}$, which is responsible for the UV absorption/emission features at room temperature. The 2D exciton ground state is the only photoemission exciton energy level available, and its longer lifetime (7 μs) is expected to be related to confinement-enhanced electron−hole exchange interaction in the *c* direction and the structural anisotropy of [CdSe] monolayer.

When Cd^{2+} is partly substituted by Mn^{2+}, a strong Mn^{2+} internal transition ($^4T_1 \rightarrow {}^6A_1$) luminescence located at 2.12 eV (584 nm) is obtained at room temperature; its sharp excitation peak overlaps with the 2D exciton emission peak, which indicates that the Mn^{2+} emission is driven by the 2D exciton ground-state transition. For $x = 0.02$, the luminescence intensity of $Cd_{1-x}Mn_xSe{\cdot}hda_{0.5}$ reaches maximum and enhances 28 times compared with that of L = *en*. When $x < 0.05$, the Mn^{2+} luminescence is a characteristic single-exponential decay process with a well-defined constant lifetime of 375 μs. ESR spectra show that Mn^{2+} substitutes the Cd^{2+} ion in the inorganic monolayer and that isolated Mn^{2+} luminescence center located in a tetragonal site in $Cd_{1-x}Mn_xSe{\cdot}hda_{0.5}$ is a key factor for their strong luminescence character (enhancement effect) compared to $Cd_{1-x}Mn_xSe{\cdot}en_{0.5}$.

Our results indicate that $Cd_{1-x}Mn_xSe{\cdot}hda_{0.5}$ is a typical 2D DMS; it has a strong Mn^{2+} luminescence due to the high-efficiency energy transfer from 2D exciton ground state which forms via strong size confinement effect in the *c* direction. Their optical properties including the UV absorption and emission, longer lifetime 2D exciton ground state, and Mn^{2+} luminescence are different from those of CdSe:Mn nanocrystals or quantum wells. And it can be speculated that the other important properties, magneto-optical effect, for example, is also unique and worth further investigation.

Acknowledgment. This work was supported by the National Natural Science Foundation of China, and the National Key Fundamental Research and Development Program of China (973 Program).

Supporting Information Available: Reitveld refinement of the structure of $CdSe{\cdot}hda_{0.5}$, structure relationship of $CdSe{\cdot}L_{0.5}$ and hexagonal CdSe, and absorption/emission spectra of $CdSe{\cdot}en_{0.5}$ (PDF). This material is available free of charge via the Internet at http://pubs.acs.org.

CM048339Y

(32) Gonzalez Beermann, P. A.; McGarvey, B. R.; Muralidharan, S.; Sung, R. C. W. *Chem. Mater.* **2004**, *16*, 915.
(33) Borse, P. H.; Srinivas, D.; Shinde, R. F.; Date, S. K.; Vogel, W.; Kulkarni, S. K. *Phys. Rev. B* **1999**, *60*, 8659.